Ab initio study of iron and iron hydride: II. Structural and magnetic properties of close-packed Fe and FeH

1998 J. Phys.: Condens. Matter 10 5113

(http://iopscience.iop.org/0953-8984/10/23/013)

J. Phys.: Condens. Matter **10** (1998) 5113–5129. Printed in the UK PII: S0953-8984(98)90979-1

Ab initio study of iron and iron hydride: II. Structural and magnetic properties of close-packed Fe and FeH

C Elsässer†‡‖, Jing Zhu†¶, S G Louie†, B Meyer‡, M Fähnle‡ and C T Chan§+

† Department of Physics, University of California, Berkeley, CA 94720, USA
‡ Max-Planck-Institut für Metallforschung, Heisenbergstrasse 1, D-70569 Stuttgart, Germany
§ Ames Laboratory and Department of Physics, Iowa State University, Ames, IA 50011, USA

Received 23 January 1998, in final form 16 March 1998

Abstract. The energetical ordering and magnetic states of hexagonal and double-hexagonal close-packed (hcp, dhcp) as well as face-centred cubic (fcc) Fe and FeH crystals are studied via spin-polarized *ab initio* total-energy calculations in the local spin-density approximation and with generalized gradient corrections by means of the mixed-basis pseudopotential and the all-electron LMTO–ASA methods. In all three structures, the magnetic spin moments go to zero under volume compression. For pure Fe in the compressed non-magnetic state, the hcp structure is found to have the lowest energy, fcc the highest, and the dhcp structure lies in between. The two hexagonal structures have significantly smaller than ideal c/a ratios. For compressed non-magnetic FeH the energetical ordering of the structures is reversed, compared to that for pure Fe, with fcc ground-state structure and almost ideal c/a ratios for both hexagonal structures. In the ferromagnetic states at expanded volumes, the energetical orderings are again opposite to those of the non-magnetic states both for Fe and FeH. In ferromagnetic FeH these energy differences are particularly small, yielding almost an energetical degeneracy of all three close-packed structures.

1. Introduction

For pure iron, a variety of crystal structures depending on the external pressure and temperature have been found and studied intensively (see, e.g., references [1] and [2]). For instance, body-centred cubic (bcc) α-Fe is transformed to hexagonal close-packed (hcp) ε-Fe at room temperature under the influence of a strong hydrostatic pressure (13.1 GPa [3, 4]). At atmospheric pressure a transition from α-Fe to face-centred cubic (fcc) γ-Fe appears at a high temperature (1200 K; see, e.g., reference [5]). Very recently, evidence was reported for a new high-pressure phase ε'-Fe with a double-hexagonal close-packed (dhcp) structure [6].

Related to the variety of crystalline structures is a very complicated magnetic behaviour with respect to external conditions. While α-Fe is known to be a ferromagnet for temperatures up to its Curie temperature (1043 K) and a paramagnet above, there is evidence for γ-Fe for ferromagnetic [7], antiferromagnetic [8] or even incommensurately arranged [9] spin structures. No magnetic ordering down to a temperature of 0.03 K has been

‖ Present address: Max-Planck-Institut für Metallforschung, Seestrasse 92, D-70174 Stuttgart, Germany.
¶ Present address: Lawrence Livermore National Laboratory, Livermore, CA 94551, USA.
+ Present address: Physics Department, Hong Kong University of Science and Technology, Clear Water Bay, Hong Kong.

0953-8984/98/235113+17$19.50

observed for the high-pressure phase ε-Fe [5]. These interesting and complicated properties of pure iron, which have been investigated intensively, for instance, by means of electronic structure theories (see, e.g., references [10–16]), provide the background for the study of iron–hydrogen systems, which is the topic of our work presented here.

Some results of experimental observations will serve to introduce the binary iron–hydrogen system: under normal conditions (room temperature and atmospheric pressure) bcc α-Fe absorbs only a very small amount of hydrogen in its crystal lattice [17]. However, this can be sufficient to cause very undesirable changes of the mechanical properties of iron, leading to material failures because of embrittlement and corrosion.

Several years ago, by application of very high external pressures or temperatures it became possible to form high-concentration stoichiometric hydride compounds of iron and some other transition metals, which absorb only few hydrogen atoms under normal conditions [18]. The capability of iron in particular to absorb H or other light elements (B, C, N, O) under extreme conditions has became a subject of great interest in geophysics in connection with the question of the constitution of the Earth's inner core.

Antonov *et al* [19] reported the formation of iron hydride at a temperature of 250 °C and a pressure of 6.7 GPa. After quenching and cooling in liquid nitrogen to −180 °C the iron hydride was found to remain metastable at atmospheric pressure. The degradation started at a temperature of −120 °C. The crystal structure was determined by x-ray diffraction to be hcp (ε-FeH). In reference [20], FeH was found to be a ferromagnet with a Curie temperature high above −180 °C. A subsequent investigation [21] addressed the determination of the $T-p$ phase diagram of the Fe–H system for temperatures up to 450 °C and pressures up to 6.7 GPa. Above 5 GPa and 300 °C, a transition from hcp FeH to presumably fcc FeH was found. More recently, Antonov *et al* [22] synthesized $FeH_{0.88}$ at 350 °C and 9 GPa. The measured x-ray spectra could be understood best by assuming a dhcp crystal structure.

By compression of iron and hydrogen together in a high-pressure cell at room temperature, Badding *et al* [23] observed a macroscopic expansion of the iron sample, directly visible to the eye, starting at a hydrostatic pressure of 3.5 GPa. The crystal structure of the expanded sample was studied by x-ray diffraction: above 3.5 GPa, additional lines, which can be attributed well again, as in reference [22], to a dhcp structure of iron atoms, appeared besides the lines of bcc α-Fe in the spectra. The lines of α-Fe disappeared gradually between 9.45 and 14.7 GPa, while the lines of the dhcp structure did not change noticeably up to the maximally applied pressure of 62 GPa. The structural change was found to be reversible and cyclically repeatable. The volume expansion at 3.5 GPa was interpreted as the formation of an almost stoichiometric $FeH_{0.94}$ compound with H atoms occupying the octahedral interstitial sites of the dhcp Fe lattice.

This dhcp structure of FeH was further supported by results of Mössbauer experiments [24, 25] which yielded signals from two crystallographically inequivalent Fe sites, a characteristic feature of the dhcp structure. Fukai *et al* [26] reported high-pressure experiments on the Fe–H system where a sequence of structural transitions, dhcp → fcc → bcc with defects → melt, was observed with increasing temperature under a pressure of 6 GPa. The fcc FeH below 650 °C was interpreted as being metastable with respect to dhcp FeH, which can be formed at room temperature [23]. Evidence for the formation of fcc $FeH_{0.13}$ under pressure was already reported earlier [27].

The quoted experimental observations give a rough picture of the Fe and Fe–H phase diagrams. However, not all findings about the crystal structure and the magnetic properties have been clarified and understood yet, leaving the Fe–H system as a challenge for further electron-theoretical studies (like the pure Fe system; see, e.g., [6, 28–31]). In the present work, part II of our *ab initio* study of iron and iron hydride (for parts I and III, see

references [32] and [33], respectively) results for the equations of state (EOS) are reported and discussed, namely the total energy and magnetic spin moment versus the unit-cell volume of iron and of stoichiometric iron monohydride in the hcp, dhcp and fcc crystal structures, with hydrogen occupying the interstitial octahedral sites of the close-packed iron lattices.

The currently available experimental information indicates that high temperatures and/or high pressures are necessary to form the various Fe and FeH structures. Not very much is known about the thermodynamic phase stability of FeH at low temperatures except that it seems to be metastable if quenched below a temperature of -120 °C [19]. Theoretical *ab initio* density-functional calculations, like ours and the ones cited above, commonly describe the quantum-mechanical ground state of the electrons and, by assuming rigid lattices for the atomic positions, neglect vibrational excitations of the ions. Hence such calculations address the high-pressure properties of materials at zero temperature. (A procedure for dealing with elevated temperatures for the bcc and hcp phase competition in Fe has been reported recently [34].)

2. Theoretical methods

To calculate the EOS for iron and iron hydride, *ab initio* total-energy methods based on the density-functional theory are applied. In particular we used the mixed-basis pseudopotential (MBPP) method [35–37] and the linear muffin-tin orbital (LMTO) method with the atomic sphere approximation (ASA) [38, 39]. The computational techniques and the approximations in the density-functional theory [40, 41] (local density or local spin-density approximation, LDA/LSDA, and generalized gradient approximations) have been summarized in part I. Here we use the MBPP method to study the structural ordering of Fe and FeH without and with spin polarization, and the LMTO–ASA method to calculate the magnetic ordering via spin polarization over a large volume range of compression and expansion around the volume for which the magnetic instability appears. This breakdown of the magnetic spin moment is typical for close-packed iron systems and has been discussed in part I for the case of fcc Fe and FeH.

All of the close-packed crystalline structures considered are described by hexagonal crystalline unit cells (Bravais lattices), with two atoms per cell for hcp (stacking sequence ABAB of close-packed atomic planes, hexagonal symmetry), three atoms per cell for fcc (ABCABC, trigonal symmetry) and four atoms per cell for dhcp (ABACABAC, hexagonal symmetry) iron.

The mixed basis of plane waves and localized orbitals used to describe the one-electron wavefunctions is given by the same cut-off parameters as in part I was used. For H a norm-conserving local pseudopotential [42] was used, and for Fe a norm-conserving, non-local, non-linear, optimally smooth ionic pseudopotential [43, 44] with the same construction parameters and properties as the PC2 pseudopotential used in part I was used, except that it has been constructed from non-relativistic instead of relativistic atomic all-electron states. This, however, is of no relevance for the calculated properties of Fe and FeH addressed in this work. For the sampling of the hexagonal-Brillouin-zone integrals, special Chadi–Cohen $\boldsymbol{k}$-points [45] with approximately the same mesh density as for the cubic cases in part I and the same Gaussian broadening [36, 46] of 0.004 Ryd have been used. The LMTO basis set used in this work, part II, contained s, p and d orbitals only. The Brillouin-zone summations were carried out using special Monkhorst–Pack $\boldsymbol{k}$-points [47] and an improved tetrahedron method [48]. (In this paper we chose to use both atomic Rydberg units and electron volts for energies, 1 Ryd = 13.606 eV. Lengths are given in ångströms or in atomic Bohr units,

1 Bohr = 0.529 Å. The atomic units are 'natural' for *ab initio* calculations; eV and Å are more convenient for comparisons with literature data.)

3. Structural properties

The structural properties of close-packed Fe and FeH were determined by calculating total energies as functions of the lattice parameters. Whereas in the fcc cases there is only one degree of freedom, which is chosen to be the unit-cell volume, in the hcp and dhcp crystals there is a second degree of freedom, which can be chosen conveniently to be the ratio c/a of the lengths of the axial and basal lattice parameters, c and a, respectively. The ideal value for close-packed hard spheres, stacked in an ABAB sequence, in the hcp structure is $(c/a)_{\mathrm{hcp}}^{\mathrm{ideal}} = \sqrt{8/3}$. Consequently, for the fcc structure represented by a hexagonal unit cell and an ABCABC sequence (and no freedom to vary without breaking the cubic symmetry), it is $(c/a)_{\mathrm{fcc}} = \frac{3}{2}(c/a)_{\mathrm{hcp}}^{\mathrm{ideal}}$. For the dhcp structure with an ABACABAC sequence, it is $(c/a)_{\mathrm{dhcp}} = 2(c/a)_{\mathrm{hcp}}$.

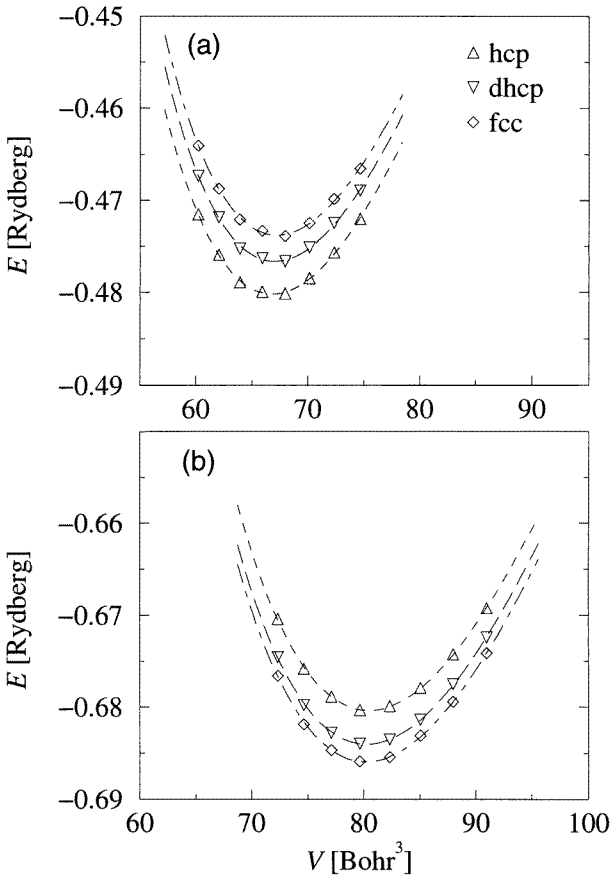

Figure 1. Equations of state calculated in the LDA (CA) using the MBPP method: (a) for NM Fe; (b) for NM FeH. The symbols mark the *ab initio* data points (calculated with the ideal c/a ratio). The lines through the symbols show the fitted EOS of Rose *et al* [49, 50].

Table 1. The cohesive parameters V_0, B_0 and B' of non-magnetic (NM) and ferromagnetic (FM) Fe with fcc, dhcp and hcp crystal structures; the δE are energy differences with respect to fcc Fe in the same magnetic state.

		NM				FM			
xc functional	Lattice structure	V_0 (Å^3)	B_0 (GPa)	B'	δE (mRyd)	V_0 (Å^3)	B_0 (GPa)	B'	δE (mRyd)
MBPP									
CA	fcc	9.95	320	4.5	0	11.38	214	4.1	0
	dhcp	9.92	324	4.5	−1.5				0.6
	hcp	9.88	324	4.5	−5.1				2.5
BP	fcc	10.71	255	4.7	0	12.44	167	4.3	0
	dhcp	10.67	258	4.7	−1.0				0.8
	hcp	10.64	258	4.7	−5.1				2.9
PW	fcc	11.03	242	4.7	0	12.80	160	4.3	0
	dhcp	11.00	245	4.7	−1.0				0.7
	hcp	10.97	245	4.7	−5.1				2.8
LMTO–ASA									
CA	fcc	9.97	324	4.6	0	11.35	193	4.0	0
	dhcp				−1.2	11.39	192	4.0	1.5
	hcp				−4.3	11.39	190	4.0	3.6
PW	fcc	10.98	244	4.9	0	12.83	152	4.3	0
	dhcp				−1.1	12.86	151	4.3	1.3
	hcp				−4.3	12.89	150	4.3	3.6
Experiment [4, 23]									
	hcp					11.18	160	5.8	

First we calculated the total energies of Fe and FeH as functions of the volumes (per Fe atom or FeH formula unit, respectively) for fixed ideal c/a ratios. Figure 1 shows the results for Fe and FeH in the three close-packed structures, obtained in the LDA without spin polarization (non-magnetic, NM) using the MBPP method. The symbols mark the *ab initio* data points $E(V)$. As discussed in detail in part I, an analytic model EOS given by Rose *et al* [49, 50] was fitted to these data to extract cohesive parameters for the crystals, namely the equilibrium volume V_0, the bulk modulus B_0 and its pressure derivative B' (equivalent to V_0, B_0 and the cohesive energy E_0; cf. part I). The lines connecting the *ab initio* data points in figure 1 are the fitted EOS. The corresponding values for the cohesive properties can be found in tables 1 and 2 (labelled MBPP, CA, NM; for the meanings, see the following paragraph).

Table 1 compiles all of the results obtained from $E(V)$ data with ideal c/a ratios for the cohesive properties of hcp, dhcp and fcc Fe, both in non-magnetic (NM) and ferromagnetic (FM) spin states, in the LSDA (using the functional of Ceperley and Alder [51], CA, in the parametrization of Perdew and Zunger [52]), and with gradient-corrected density functionals given by Perdew and Wang [53–55] (PW) and by Becke [56] and Perdew [53, 54] (BP) (for details we refer the reader to part I), using the MBPP and the LMTO–ASA methods. Table 2 contains a compilation of corresponding results for FeH.

From the data given in tables 1 and 2 and in figure 1 it is easy to calculate the volume dependence of the hydrostatic pressure, $p(V) = -\mathrm{d}E/\mathrm{d}V$, or the pressure dependence of

Table 2. The cohesive parameters V_0, B_0 and B' of non-magnetic (NM) and ferromagnetic (FM) FeH with fcc, dhcp and hcp crystal structures; the δE are energy differences with respect to fcc Fe in the same magnetic state.

		NM				FM			
xc functional	Lattice structure	V_0 (Å^3)	B_0 (GPa)	B'	δE (mRyd)	V_0 (Å^3)	B_0 (GPa)	B'	δE (mRyd)
MBPP									
CA	fcc	11.87	298	4.1	0	12.38	197	3.6	0
	dhcp	11.88	297	4.1	1.1				−1.2
	hcp	11.91	294	4.1	3.9				−1.9
BP	fcc	12.69	248	4.3	0	13.89	155	3.7	0
	dhcp	12.69	248	4.3	1.9				−0.3
	hcp	12.73	246	4.3	4.0				−0.9
PW	fcc	13.05	236	4.3	0	14.36	147	3.7	0
	dhcp	13.06	236	4.3	1.8				−0.5
	hcp	13.09	234	4.3	3.7				−1.2
LMTO–ASA									
CA	fcc	11.92	296	4.2	0	12.63	211	3.7	0
	dhcp				1.9	12.55	218	3.8	−1.6
	hcp				5.6	12.54	228	3.8	−1.7
PW	fcc	13.04	233	4.4	0	14.20	165	4.0	0
	dhcp				1.6	14.08	162	3.9	−0.4
	hcp				5.0	14.05	164	3.9	−0.3
Experiment [23]									
	dhcp					13.90	121	5.3	

the volume, $V(p)$, by differentiating analytically the EOS of Rose *et al*, and hence to obtain the enthalpy, $H(p) = E + pV$, of the ground state of a crystal ($T = 0$ K).

Small density-functional total-energy differences between crystals with close-packed lattices, which are only distinguished by different stacking sequences of atomic planes, were found to be computable very accurately, as demonstrated for instance in calculations of stacking-fault energies of noble metals [57–59]. Such energy differences δE, which allow for conclusions about the mutual relative stability of crystals in their ground states ($T = 0$ K), were calculated for the three close-packed structures of Fe and FeH. The results are included in tables 1 and 2. Looking at these energy differences δE, we notice that the LDA/LSDA and gradient corrections yield very similar results for both the Fe and FeH cases within a few tenths of a millirydberg for differences of a few millirydbergs, using both MBPP and LMTO–ASA methods. (We estimate the numerical accuracy of these tiny energy differences to be better than approximately 0.5 mRyd in the MBPP method and, under the constraint of ideal c/a ratios, in the LMTO–ASA method as well.)

For pure NM Fe these results yield the hcp structure to be theoretically most stable over the whole volume range considered, in particular at compressed volumes. This is compatible with the experimental observation of non-magnetic ε-Fe at room temperature under a hydrostatic pressure of more than 13.1 GPa [23]. The fcc structure has the highest energy, and the dhcp structure lies in between. This is rather plausible, because the dhcp structure consists of two alternating close-packed atomic planes, one with nearest-neighbour

surroundings like in the hcp structure, the other like in the fcc structure.

For stoichiometric NM FeH the energetical order of the three structures turns out to be just reversed, with fcc FeH the most stable, hcp FeH the least stable and dhcp FeH in between. This discrepancy compared with the experimental observation for dhcp FeH under pressure above 3.5 GPa at room temperature [23] can be attributed to the constraints of ideal c/a ratios and ideal octahedral H positions for dhcp FeH in the calculations made so far. Below, both calculational constraints will be removed. The energy order of the close-packed structures with ideal c/a ratios for NM Fe and FeH remains unchanged over the whole volume range considered (corresponding to pressures between -40 and $+100$ GPa).

An attempt to make a direct determination of the structural-transition pressures in the one-component Fe system, e.g. from bcc α-Fe to hcp ε-Fe, is hampered by the well-known problem that the close-packed NM crystal structures at their equilibrium volumes are slightly more stable than the bcc FM α-Fe in the LSDA (see part I). Hence the resulting LSDA transition pressures are not realistic. This is not only the case because of their negative values related to the lower energetical stability of α-Fe. Quantitatively there is an obvious underestimation of the equilibrium volumes, and the curvatures of the EOS which are characterized by considerably too large bulk moduli, are overestimated compared to experiment (cf. table 1 in part I). The use of gradient corrections at least corrects the stability ratio between α-Fe and γ-Fe but still leaves noticeable quantitative discrepancies between calculated and experimental results (see tables 1 here and in part I).

A determination of structural-transition pressures in the two-component Fe-H system, e.g. from bcc α-Fe and liquid H_2 to dhcp FeH, is further complicated by the need for a common zero-energy level. In principle this can be defined as the energy of the total system separated into spatially widely separated, single atoms. This is the energy which the cohesive energies E_0 are referred to. However, these E_0-values are considerably underestimated in the LDA, compared to experimental data, by several tenths of an eV, which may cause transition pressures to deviate from experiment by some orders of magnitude (see, e.g., reference [60]). Again the gradient-corrected density functionals resolve the discrepancies partly, but still considerable deviations of theory from experiment remain.

Because of this concern, we gave up reporting serious estimates of critical pressures for transitions from α-Fe to close-packed structures of Fe or FeH in this work and confined our study to the energetic ordering of the three close-packed structures only.

Badding *et al* [23] determined the EOS by measuring the volume as a function of the hydrostatic pressure and by subsequently fitting an EOS to the measured data points. For the close-packed high-pressure structures of Fe (above 13.1 GPa [3, 4, 23]) and FeH (above 14.7 GPa [23]) the cohesive properties V_0, B_0 and B' quoted as experimental data in tables 1 and 2 were extracted using the Vinet *et al* EOS [61, 62] for $V(p)$ which is just the inversion of the analytic derivative $p(V) = -\mathrm{d}E/\mathrm{d}V$ of the Rose *et al* EOS [49, 50]. In figure 2 we plot the theoretical NM results for $p(V)$ for Fe and FeH obtained from the $E(V)$ data in the LDA without spin polarization shown in figure 1 and the corresponding gradient-corrected $E(V)$ data. In this kind of plot the curves for the three close-packed structures are almost indistinguishable. The curves obtained in the LDA and with gradient corrections are very similar in shape and are only shifted because of the increase of V_0 by the gradient corrections. The shapes of these curves are rather insensitive to the related relatively large decreases of B_0 and to the increases of B' when going from the LDA to the gradient-corrected LDA. The lines of crosses starting at $p = 0$ in figure 2 mark the shape of the EOS of Vinet *et al* as obtained by using the cohesive properties quoted in reference [23] (cf. tables 1 and 2), which were determined by fitting to experimental high-pressure data (with an extrapolation of the EOS from 13.1 and 14.7 GPa to zero pressure for Fe and

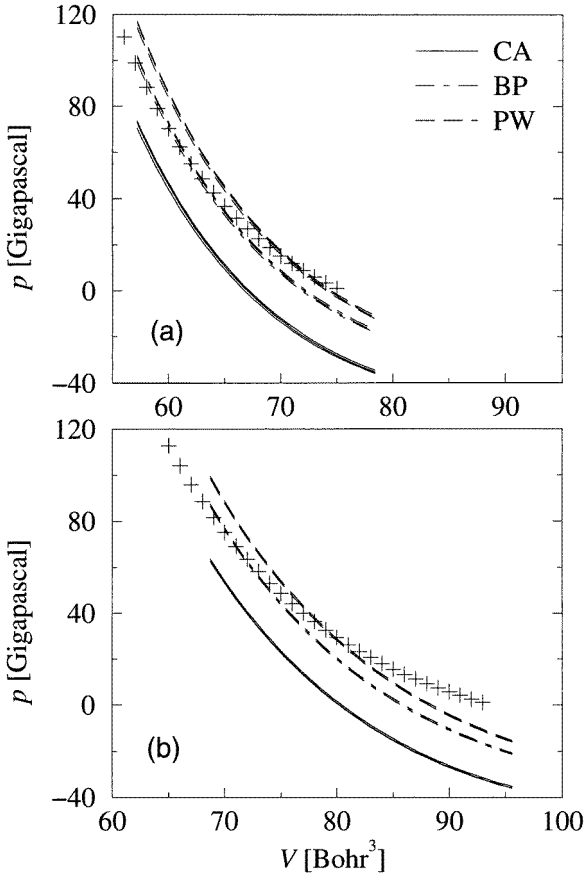

Figure 2. Pressure–volume curves derived from the EOS of Rose *et al* fitted to non-spin-polarized *ab initio* MBPP $E(V)$ data (cf. figure 1): (a) for NM Fe; (b) for NM FeH. Three parallel lines belonging to fcc, dhcp and hcp structures are almost indistinguishable in all three cases of density-functional approximations. The + symbols mark the EOS of Vinet *et al* fitted to experimental data.

FeH, respectively).

These 'experimental' EOS show clear deviations from the theoretical curves for all three density-functional approximations. The deviations are strongest at small pressures. One reason for this discrepancy may be the fact that at low pressures (below 13.1 and 14.7 GPa for Fe and FeH, respectively) in experiment the samples are not yet formed in single phases, namely hcp Fe or dhcp FeH, but still contain certain volume parts of bcc α-Fe. Another reason is that the theoretical data discussed so far do not include spin polarization, whereas the experimental samples are reported to be magnetically ordered to some extent. Pure close-packed Fe might be ferromagnetically ordered at very low temperature and zero pressure but is non-magnetic at room temperature, at which the experiments of Badding *et al* were done [23]. Close-packed FeH was found to be ferromagnetically ordered even at room temperature [24, 25]. Therefore the 'experimental' EOS has to be also compared to theoretical curves obtained from spin-polarized calculations. To reduce the computational effort, we made use of the results given in tables 1 and 2 indicating that the theoretical

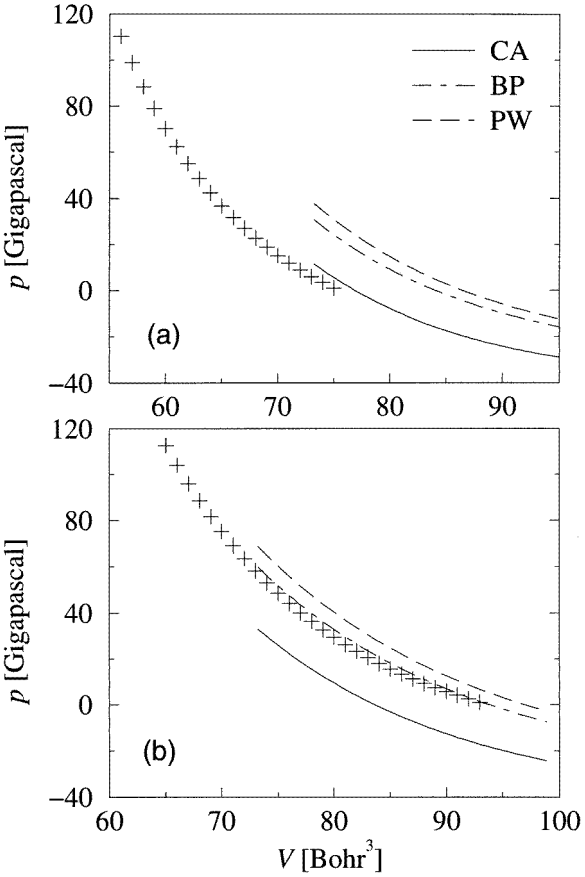

Figure 3. Pressure–volume curves derived from the EOS of Rose *et al* fitted to spin-polarized *ab initio* MBPP $E(V)$ data: (a) for FM fcc Fe; (b) for FM fcc FeH. The + symbols mark the EOS of Vinet *et al* fitted to experimental data.

results for the cohesive properties V_0, B_0 and B' of all three close-packed structures, for both non-magnetic and ferromagnetic states as well as both for Fe and for FeH, are almost identical. This allows us to set the 'experimental' EOS of hcp Fe and of dhcp FeH in direct comparison with the theoretical EOS obtained for spin-polarized fcc Fe and fcc FeH. These results for ferromagnetic fcc Fe and FeH listed in tables 1 and 2 do indeed agree better than the non-polarized results with the quoted parameters derived from experimental data. This is illustrated in figure 3 where the 'experimental' EOS, again marked with crosses, and the theoretical EOS for fcc FM Fe and FeH are plotted together. The theoretical curves end approximately at the volume at which the instability of the magnetic spin moments in fcc Fe and FeH upon compression appears (cf. figures 1(b) and 5(b) in part I).

For the pure FM Fe (see figure 3(a)), the curvatures of the calculated EOS match considerably better with the 'experimental' curve because the calculated B_0-values are much smaller and hence closer to the experimental parameter of 160 GPa. While the V_0-value in the LSDA is close to the experimental parameter of 11.18 Å^3 and leads to an almost smooth merging of the theoretical LSDA EOS into the 'experimental' EOS, the gradient-corrected EOS are shifted because of the larger theoretical V_0-values. However, in the LSDA

as well as in the gradient-corrected calculations the ferromagnetic ordering has already broken down at rather small pressures. From this discussion we conclude for pure Fe that, perhaps, the high-pressure EOS is roughly described by the theoretical NM results because theoretically the FM solutions have already vanished at low pressures and experimentally the sample is reported to be non-magnetic at room temperature and pressures above 13.1 GPa (where the coexisting magnetic bcc phase has vanished). The NM results obtained with the BP functional might give quantitatively a slightly better theoretical description of the experimentally observed EOS than the results for the LDA and PW functionals. This may be seen as a justification of earlier theoretical studies of the high-pressure EOS of Fe, in which no spin polarization was accounted for in the hcp or dhcp phases of Fe [28, 31, 34].

For the FM FeH, on the other hand, figure 3(b) shows a rather large pressure range over which a theoretical FM solution remains stable. Here again the curvatures of the theoretical EOS follow rather well the experimental EOS because the B_0-values are considerably smaller than in the NM case, and hence are closer to the experimental value of 121 GPa. The V_0-value in the LSDA is smaller than the experimental parameter of 13.90 Å^3. The gradient-corrected V_0-values, in particular the BP value, are much closer to this. Altogether, for FeH under hydrostatic pressure we conclude that the theoretical results seem to indicate the importance of a magnetic ordering for the understanding of the EOS. Again, closest to the 'experimental' EOS lie the theoretical BP results for FM FeH up to the pressure at which the magnetic ordering vanishes in theory (roughly 60 GPa; see figure 3(b)) and for NM FeH above this pressure (see figure 2(b)). This is compatible with the experimental result that the FeH sample was found to be ferromagnetic up to high pressures at room temperature. But we recall that the agreement between the theoretical results, both in the LDA and including gradient corrections, and the experimental data for the EOS of Fe and FeH under external pressures is quantitatively not very good.

So far, all of the theoretical results were obtained under the constraint of ideal c/a ratios. In qualitative disagreement with experiment, the fcc structure was found to be more stable than the dhcp structure for FeH. To estimate the influence of this second degree of freedom in the hcp and dhcp lattices on the energetical ordering of the three close-packed structures, we calculated the total energy as a function of c/a with the unit-cell volumes fixed at the calculated equilibrium values V_0 for the ideal c/a ratios for NM Fe and FeH (cf. tables 1 and 2). The results are displayed in figure 4. First, as is to be expected for a cubic crystal, for Fe and FeH calculated using a hexagonal unit cell with three Fe layers in the ABC stacking sequence and imposing only the 12 symmetry operations of the trigonal space group D^3_{3d}, the energy minima turn out to be very accurately at the ideal ratio $(c/a)_{fcc} = \frac{3}{2}\sqrt{8/3}$ of the fcc lattice. (The hcp and dhcp crystals have the hexagonal space group D^4_{6h} with 24 symmetry operations.) Test calculations yielded the result that this may be not the case if the $\boldsymbol{k}$-point mesh used for Brillouin-zone sampling is not chosen sufficiently dense. Second, for pure Fe we find a significantly lower energy of approximately -0.5 mRyd for hcp Fe with $(c/a)_{hcp} = 1.59$, and a slightly lower energy less than -0.1 mRyd for dhcp Fe with $(c/a)_{dhcp} = 3.24$, both in good accordance with experimental data for temperatures at which the specimens were paramagnetic (1.60 for hcp ε-Fe [3, 4], 3.23 for dhcp ε'-Fe [6]) and *ab initio* full-potential LMTO calculations (1.585 for hcp and 3.234 for dhcp [31]). Third, for FeH the c/a ratios are found to be equal to the ideal ratios within a relative numerical accuracy of 0.2% for both hcp and dhcp lattices.

For both Fe and FeH, the dhcp structure is energetically closer to the fcc structure, separated by only approximately 1 mRyd, than to the hcp structure. Considering the dhcp structure as a fcc structure with the highest possible concentration of extrinsic stacking faults, the close-packed FeH can be interpreted in theory as a material with a ground-state

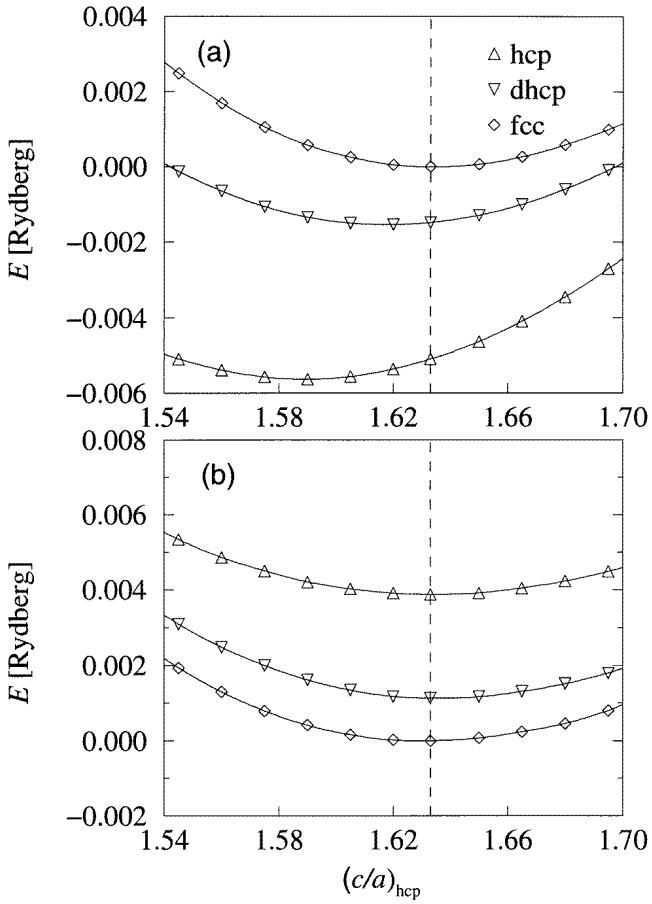

Figure 4. Total energies as function of $(c/a)_{\rm hcp} = \frac{2}{3}(c/a)_{\rm fcc} = \frac{1}{2}(c/a)_{\rm dhcp}$ at constant V_0, calculated with the ideal c/a ratio in the LDA (CA) using the MBPP method (cf. figure 1): (a) for NM Fe, (b) for NM FeH. The energy zero is set to the energy of the fcc crystals (with the ideal c/a ratio related to the cubic symmetry) The symbols mark the *ab initio* data points. The solid lines connecting the data points are cubic splines. The vertical dashed lines mark the ideal c/a ratio for close-packed structures.

fcc structure and a very small stacking-fault energy. Because of this small defect energy and the almost ideal c/a ratios, it seems to be not unlikely to find coexisting regions with fcc and dhcp stacking sequences in real samples under extreme external conditions. However, the theoretical c/a relaxation only weakens and does not remove the qualitative discrepancy with respect to experiments, where evidence for the stability of the dhcp (not the fcc) structure was found. In the close-packed pure Fe, on the other hand, the theoretical ground-state hcp structure is energetically stronger, preferred over the dhcp and fcc structures (separated from the dhcp sructure by about 4 mRyd). This and the considerable deviation of the c/a from the ideal ratio make it seem less likely that the other two stacking sequences will form, at least for the NM equilibrium volume considered, V_0. However, recent high-pressure experiments gave strong evidence for the existence of dhcp ε'-Fe at high pressure and temperature [6].

In principle, V_0 and c/a should be varied iteratively to determine the equilibrium hcp and dhcp structures. However, the results described above show that for both hcp and dhcp

FeH, total-energy minima are already found for the ideal c/a ratios (see figure 4(b)). For pure Fe, on the other hand, a further energy lowering by a subsequent volume relaxation for the calculated non-ideal c/a ratios given above (see figure 4(a)) is expected for hcp Fe and, to a lesser extent, also for dhcp Fe. However, these volume relaxations will only increase the fcc–dhcp–hcp energy differences by a small amount. But the energetical ordering found for the three structures cannot be changed because the energetically highest, fcc, structure has no possibility of relaxing, and the deviation of the ideal c/a ratio for the energetically intermediate, dhcp, structure is already smaller than that of the energetically lowest, hcp, structure.

One further structural degree of freedom exists just for FeH in the dhcp structure: the H atoms at the octahedral interstitial sites are allowed to shift along the hexagonal c-axis, by the same amounts but in opposite directions from H to H, without changing the hexagonal space group of the dhcp structure. This causes another small energy lowering of the dhcp structure, which, however, is calculated to be less than 0.3 mRyd per FeH formula unit and thus may not change any conclusions. (The calculated extent of the optimum displacement of the H atoms away from the ideal octahedral sites along the c-axis is 0.04 Å or 2% of the mutual H–H distances.)

4. Magnetic properties

In the present section, the possibility of spin polarization is always included in the calculations of total energies E and magnetic spin moments μ as functions of the volumes V (with ideal c/a ratios) to describe the EOS of Fe and FeH over a wide volume of compression and expansion. According to the data given in tables 1 and 2, the cohesive properties for fcc Fe and FeH and the energy differences δE between the three close-packed structures calculated using the MBPP and the LMTO–ASA methods with or without spin polarization agree very well. Therefore, only the results obtained with the LMTO–ASA and spin-polarized density functionals are presented here. (In the cases of the FM MBPP and NM LMTO–ASA methods, the energy differences δE given in tables 1 and 2 were obtained for hcp and dhcp structures by using the calculated V_0 of the fcc structure. This is justified by the almost equal values of V_0 for all three structures in the other cases, those of the NM MBPP and FM LMTO–ASA methods.)

In parallel with all of the LSDA calculations reported in this section, corresponding calculations with PW gradient correction were performed. The energetical orderings of all of the structures considered were found to be the same (see tables 1 and 2), as were the volume dependences of the magnetic spin moments.

Figures 5(a) and 6(a) show the $E(V)$ LSDA results for Fe and FeH, respectively. The symbols mark the *ab initio* data points. For a better illustration, only the hcp data points are connected by segments of straight solid lines as guides to the eye. Fits of EOS to these $E(V)$ data over the whole volume ranges are not useful because of the magnetic instability which is visible in the $E(V)$ curves between 75 and 80 Bohr^3. For volumes smaller than 75 Bohr^3 the LMTO–ASA results, which were obtained in the LSDA, correspond to and agree well with the NM MBPP results (see figure 1), except for a volume-independent energy shift due to differences in E_0 (cf. tables 1 and 2 in part I). Above 80 Bohr^3 the ferromagnetically ordered states are stable. Figures 5(b) and 6(b) show the corresponding $\mu(V)$ results with the obvious breakdown of magnetic ordering. (At the V_0-values quoted in table 1, obtained from fits of the Rose *et al* EOS to the FM $E(V)$ with $V > 75$ Bohr^3, the FM states of Fe are found to be unstable with respect to NM states in the LSDA calculation, but stable in the gradient-corrected PW calculation; cf. figures 5(a) and 7.)

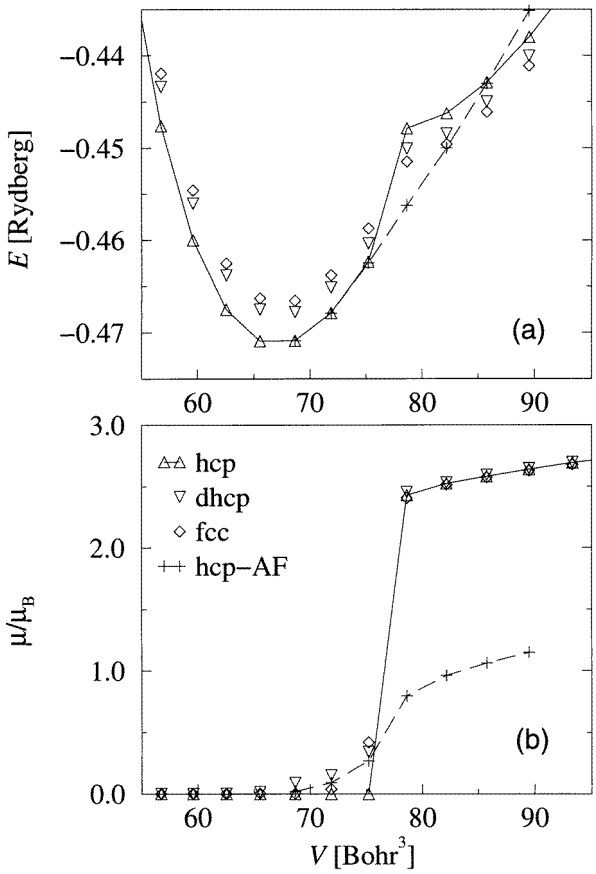

Figure 5. (a) Total energies E and (b) magnetic spin moments μ per Fe atom as functions of the volume V for Fe calculated in the LSDA (CA) by the spin-polarized LMTO–ASA method. The symbols mark the *ab initio* data points. The FM and AF hcp data points are connected by straight pieces of solid and dashed lines, respectively, for better illustration.

From figures 5 and 6, the following can be stated for the magnetic behaviour of Fe and FeH: the energetical orderings of the three close-packed lattices in magnetically ordered states are just the opposite of those for the non-magnetic states.

For pure Fe in the LSDA (see figure 5) this means that at small volumes, which can be reached for instance by applying high external pressures, the NM hcp structure is the most stable. This result of the LSDA of the theoretical magnetic ground state ($T = 0$ K) is in accordance with the experimental observation that hcp ε-Fe is not magnetically ordered at low temperatures [18]. The use of the gradient-corrected PW functional yields that for high pressures the energetic stability of the NM hcp structure over the FM hcp structure is substantially reduced and vanishes towards zero pressure. The gradient correction shifts the $E(V)$ curves of the FM states to lower energies, as shown in figure 7. The energetical orderings of the three close-packed structures in each non-magnetic or ferromagnetic state, however, are not affected by the gradient correction. At large volumes the FM fcc structure is preferred. Such volume expansions could perhaps be achieved to some extent by lattice expansions via alloying of Fe with some other elements, or via very high temperatures. However, under the latter conditions the thermal energy would be large compared to the

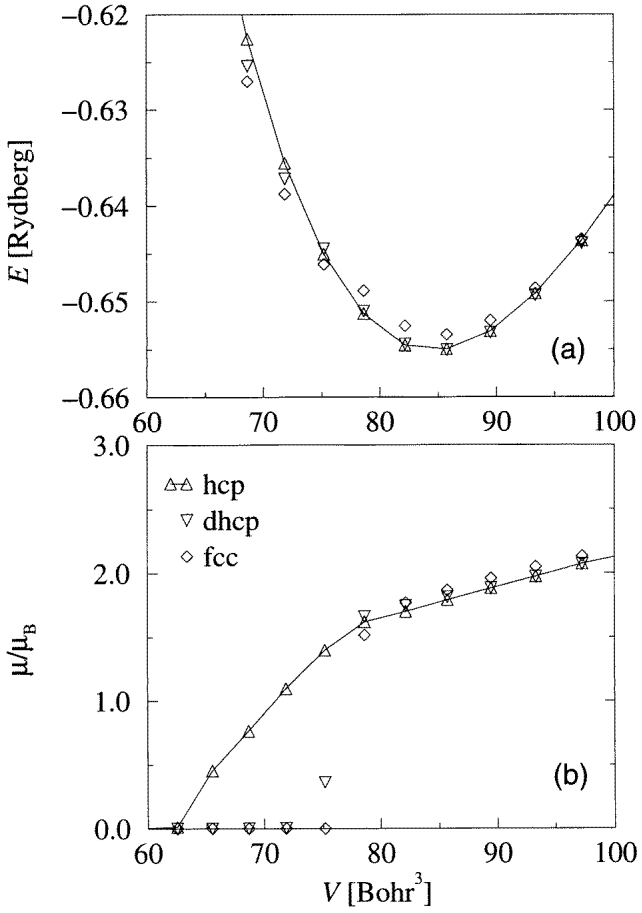

Figure 6. (a) Total energies E and (b) magnetic spin moments μ per Fe atom as functions of the volume V for FeH calculated in the LSDA (CA) with the spin-polarized LMTO–ASA method. The symbols mark the *ab initio* data points. The FM hcp data points are connected by straight pieces of solid lines for better illustration.

structural energy differences and the exchange energy stabilizing the magnetic states, and thus for a distinct preference of the fcc structure, differences in free enthalpies instead of total energies need to be considered. In the volume range between 75 and 80 Bohr^3 an antiferromagnetically ordered hcp structure with spin moments of about 1 μ_B on the two sublattices is found to be most stable. Such an antiferromagnetic ordering has been found and discussed in previous *ab initio* studies, in most detail for fcc Fe [10–13], but also for hcp Fe [14]. The latest studies report the existence of non-collinear spin arrangements in this volume range with even lower energies [15, 16].

For FeH (see figure 6) the structural energy differences in the LSDA are significantly reduced by the magnetic ordering. The three close-packed structures at expanded volumes are energetically almost degenerate, within about 1 mRyd. Slightly larger but still very small energy differences are found by including the PW gradient correction, as shown in figure 8. For FeH, again, differences of free enthalpies, not total energies, should be calculated to decide on the most stable close-packed structure at 'thermally expanded' volumes.

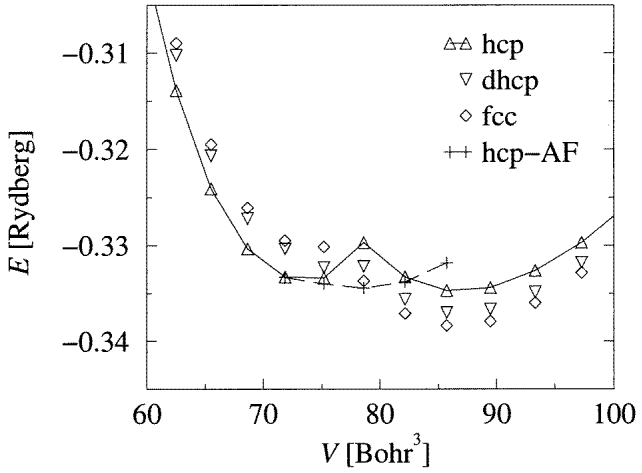

Figure 7. Total energies E per Fe atom as a function of the volume V for Fe calculated using the PW gradient correction and the spin-polarized LMTO–ASA method. The symbols mark the *ab initio* data points. The FM and AF hcp data points are connected by straight pieces of solid and dashed lines, respectively, for better illustration.

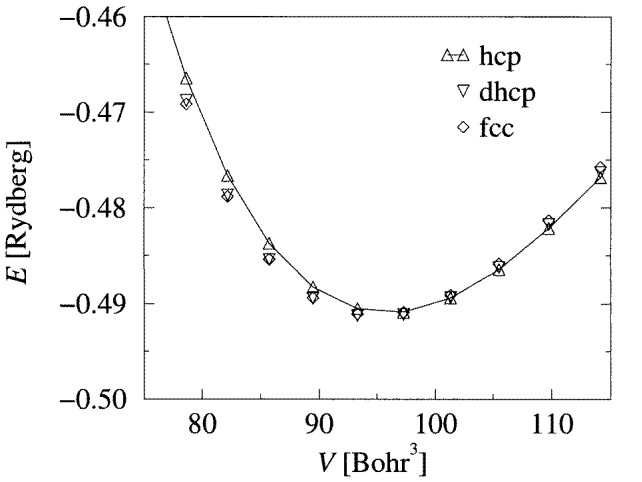

Figure 8. Total energies E per Fe atom as a function of the volume V for FeH calculated using the PW gradient correction and the spin-polarized LMTO–ASA method. The symbols mark the *ab initio* data points. The FM hcp data points are connected by straight pieces of solid lines for better illustration.

In fcc and dhcp FeH, like in all three structures of pure Fe, the magnetic spin moments change under compression from about 1.6 μ_B to zero very abruptly at around 75 Bohr^3. The hcp FeH shows a distinctly different behaviour of the breakdown of the magnetic ordering. Its magnetic spin moment decreases almost linearly from 1.6 μ_B at 80 Bohr^3 to zero over a broad range of volumes. Currently we do not know of an explanation for this peculiar behaviour. It may be related to the observation in Mössbauer experiments that close-packed FeH, unlike pure ε-Fe, seems to remain magnetically ordered up to high external pressures.

5. Summary

In this work the energetical ordering and magnetic states of close-packed crystal structures of Fe and FeH were studied via spin-polarized *ab initio* total-energy calculations in the LSDA and with generalized gradient corrections by means of the mixed-basis pseudopotential method and the all-electron LMTO–ASA method.

In all three close-packed structures considered, hcp, dhcp and fcc, of Fe and FeH, the magnetic spin moments go to zero under volume compression. For pure Fe in the compressed non-magnetic state, the hcp structure was found to have the lowest energy. The fcc structure has the highest energy, and the dhcp structure lies in between. The two hexagonal structures have significantly smaller than ideal c/a ratios. For compressed non-magnetic FeH the energetical ordering of the structures is reversed, compared to that of pure Fe, with a fcc ground-state structure and almost ideal c/a ratios for both hexagonal structures. In the ferromagnetic states at expanded volumes, the energetical orderings are again opposite to those of the non-magnetic states both for Fe and for FeH. In ferromagnetic FeH, these energy differences are particularly small, yielding almost an energetical degeneracy of all three close-packed structures.

Acknowledgments

The present work was initiated during a research year for CE at the UC Berkeley. CE gratefully acknowledges the financial support of the Max Planck Society and the hospitality at Berkeley. This work was supported in part by the National Science Foundation (UC Berkeley: Grant No DMR-9520554) and the US Department of Energy (UC Berkeley: Contract No DE-AC03-76SF00098; Ames Laboratory: Contract No W-7405-ENG-82), including computer time at the NERSC in Livermore and the NCSA in Urbana–Champaign. CE, CTC and MF are grateful for the financial support of the NATO collaborative research grant No 910439.

References

[1] Saxena S K, Dubrovinsky L S, Häggkvist P, Cerenius Y, Shen G and Mao H K 1995 *Science* **269** 1703
[2] Yoo C S, Akella J, Campbell A J, Mao H K and Hemley R J 1995 *Science* **270** 1473
[3] Mao H K, Bassett W A and Takahashi T 1967 *J. Appl. Phys.* **38** 272
[4] Mao H K, Wu Y, Chen L C and Shu J F 1990 *J. Geophys. Res.* B **95** 21 737
[5] *Landolt–Börnstein New Series* 1987 Group III, vol 19a (Berlin: Springer)
[6] Yoo C S, Söderlind P, Moriarty J A and Cambell A J 1996 *Phys. Lett.* **214A** 65
[7] Murayama H 1986 *J. Phys. Soc. Japan* **55** 2834
[8] Tsunoda Y, Imada S and Kunitami N 1988 *J. Phys. F: Met. Phys.* **18** 1421
[9] Tsunoda Y 1989 *J. Phys.: Condens. Matter* **1** 10 427
[10] Kübler J 1981 *Phys. Lett.* **81A** 81
[11] Moruzzi V L, Marcus P M, Schwarz K and Mohn P 1986 *Phys. Rev.* B **34** 1784
[12] Moruzzi V L, Marcus P M and Pattnaik P C 1988 *Phys. Rev.* B **37** 8003
[13] Moruzzi V L, Marcus P M and Kübler J 1989 *Phys. Rev.* B **39** 6957
[14] Kübler J 1989 *Solid State Commun.* **72** 631
[15] Mryasov O N, Gubanov V A and Liechtenstein A I 1992 *Phys. Rev.* B **45** 12 330
[16] Uhl M, Sandratskii L M and Kübler J 1994 *Phys. Rev.* B **50** 291
[17] Krüger J, Kunze H-D and Schürmann E 1976 *Gase und Kohlenstoff in Metallen* ed E Fromm and E Gebhardt (Berlin: Springer) p 578
[18] Ponyatovskii E G, Antonov V E and Belash I T 1982 *Sov. Phys.–Usp.* **25** 596
[19] Antonov V E, Belash I T, Degtyareva V F, Ponyatovskii E G and Shryaev V I 1980 *Sov. Phys.–Dokl.* **25** 490

[20] Antonov V E, Belash I T, Ponyatovskii E G, Thiessen V G and Shryaev V I 1981 *Phys. Status Solidi* a **65** K43
[21] Antonov V E, Belash I T and Ponyatovsky E G 1982 *Scr. Metall.* **16** 203
[22] Antonov V E, Belash I T, Degtyareva V F, Ponomarev B K and Shektman V S 1989 *Int. J. Hydrogen Energy* **14** 371
[23] Badding J V, Hemley R J and Mao H K 1991 *Science* **253** 421
[24] Choe I, Ingalls R, Brown J M, Sato-Sorensen Y and Mills R 1991 *Phys. Rev.* B **44** 1
[25] Schneider G, Baier M, Wordel R, Wagner F E, Antonov V E, Ponyatovsky E G, Kopilovskii Y and Makarov E 1991 *J. Less-Common Met.* **172–174** 333
[26] Fukai Y, Yamakata M and Yagi T 1993 *Z. Phys. Chem., NF* **179** 119
[27] Fukai Y, Fukizawa A, Watanabe K and Amano M 1982 *Japan. J. Appl. Phys.* **21** L318
[28] Stixrude L, Cohen R E and Singh D J 1994 *Phys. Rev.* B **50** 6442
[29] Stixrude L and Cohen R E 1995 *Geophys. Res. Lett.* **22** 125
[30] Stixrude L and Cohen R E 1995 *Science* **267** 1972
[31] Söderlind P, Moriarty J A and Wills J H 1996 *Phys. Rev.* B **53** 14 063
[32] Elsässer C, Zhu J, Louie S G, Fähnle M and Chan C T 1998 *J. Phys.: Condens. Matter* **10** 5081
[33] Elsässer C, Krimmel H, Fähnle M, Louie S G and Chan C T 1998 *J. Phys.: Condens. Matter* **10** 5131
[34] Moroni E G and Jarlborg T 1996 *Europhys. Lett.* **33** 223
[35] Louie S G, Ho K-M and Cohen M L 1979 *Phys. Rev.* B **19** 1774
[36] Fu C-L and Ho K-M 1983 *Phys. Rev.* B **28** 5480
[37] Elsässer C, Takeuchi N, Ho K M, Chan C T, Braun P and Fähnle M 1990 *J. Phys.: Condens. Matter* **2** 4371
[38] Andersen O K 1975 *Phys. Rev.* B **12** 3060
[39] Andersen O K and Jepsen O 1984 *Phys. Rev. Lett.* **53** 2571
[40] Hohenberg P and Kohn W 1964 *Phys. Rev.* **136** B864
[41] Kohn W and Sham L J 1965 *Phys. Rev.* **140** A1133
[42] Ho K M, Elsässer C, Chan C T and Fähnle M 1992 *J. Phys.: Condens. Matter* **4** 5189
[43] Vanderbilt D 1985 *Phys. Rev.* B **32** 8412
[44] Louie S G, Froyen S and Cohen M L 1982 *Phys. Rev.* B **26** 1738
[45] Chadi D J and Cohen M L 1973 *Phys. Rev.* B **8** 5747
[46] Elsässer C, Fähnle M, Chan C T and Ho K M 1994 *Phys. Rev.* B **49** 13 975
[47] Monkhorst H J and Pack J D 1976 *Phys. Rev.* B **13** 5188
[48] Blöchl P E, Jepsen O and Andersen O K 1994 *Phys. Rev.* B **49** 16 223
[49] Rose J H, Ferrante J and Smith J R 1981 *Phys. Rev. Lett.* **47** 675
[50] Rose J H, Smith J R, Guinea F and Ferrante J 1984 *Phys. Rev.* B **29** 2963
[51] Ceperley D M and Alder B J 1980 *Phys. Rev. Lett.* **45** 566
[52] Perdew J P and Zunger A 1981 *Phys. Rev.* B **23** 5048
[53] Perdew J P 1986 *Phys. Rev.* B **33** 8822
[54] Perdew J P 1986 *Phys. Rev.* B **34** 7406 (erratum to [53])
[55] Perdew J P and Wang Y 1986 *Phys. Rev.* B **33** 8800
[56] Becke A D 1988 *Phys. Rev.* A **38** 3098
[57] Schweizer S, Elsässer C, Hummler K and Fähnle M 1992 *Phys. Rev.* B **46** 14 270
[58] Fähnle M, Schweizer S, Elsässer C and Seeger A 1993 *Computer Aided Innovation of New Materials II* ed M Doyama, J Kihara, M Tanaka and R Yamamoto (Amsterdam: Elsevier)
[59] Schweizer S, Elsässer C and Fähnle M 1993 *Phys. Rev.* B **48** 14 706
[60] Pfrommer B 1992 *Diplomarbeit* Universität Stuttgart
[61] Vinet P, Ferrante J, Smith J R and Rose J H 1986 *J. Phys. C: Solid State Phys.* **19** L467
[62] Vinet P, Rose J H, Ferrante J and Smith J R 1989 *J. Phys.: Condens. Matter* **1** 1941